Progress In Electromagnetics Research, PIER 20, 125–151, 1998

THE LOWER- AND HIGHER-ORDER PERTURBATION EFFECTS OF A BIISOTROPIC CHIRAL SPHERE IN CYLINDRICAL AND SPHERICAL CAVITIES

W. Y. Yin

The Department of Electrical Engineering
Duisburg University
Bismarckstrasse 81
47048, Duisburg
Germany

1. Introduction
2. Geometry
3. Field Equations for the Cylindrical Cavity
3.1 The Magnetic Mode Case (TE)
3.2 The Electric Mode Case (TM)
4. The Case of Spherical Cavity
5. Numerical Results and Remarks
6. Conclusion
Appendices
References

1. INTRODUCTION

More recently, much attention has been focused on the area of electromagnetic wave propagation, scattering, radiation, and guidance in biisotropic chiral media owing to their diverse and potential applications for fabricating novel chirowaveguides, chiro-shifters, chirolenses, chiral fibers, and chiral shielding, etc., [1–4]. Biisotropic chiral materials exhibit intrinsic handedness in their interaction with electromagnetic waves, and being extra parameter presented by chirality, it permits to design devices possessing better characteristics than those of their dielectric counterparts. It is expected that as applications of chirality

in the 1–100 GHz range become practical, and naturally, much work remains to be done on characterizing the transmission characteristics as well as constitutive parameters of various chiral media. Till now, several authors have presented studies on the constitutive characteristics of artificial chiral composites theoretically. For example, the single scattering theory, full-wave method, and other approaches have been used by Luebbers and Whites, et al. to calculate the effective chirality parameter of a composite chiral material over a wide frequency band, respectively [5–9]. The macroscopic effective medium theory under Rayleigh approximation and renormalization method have been developed by Lakhtakia, Sihvola, Zhuck, and Omar more recently to evaluate the effective parameters of a disordered random biisotropic chiral medium [10–12]. Furthermore, to be able to determine the medium parameter of the biisotropic chiral material is of great importance for practical applications, and some measurement techniques have also been proposed and experimental work has been carried out to obtain material parameters of chiral composites by Hollinger, Ro, Varaden, and Guerin, et al. [13–16]. The free-space and short-waveguide techniques have been suggested to measure the chirality parameter by Tretyakov, Engheta, et al. [17, 18]. On the other hand, cavity and waveguide perturbation techniques can also give ways to determine chirality and nonreciprocity parameters [19–22] . For isotropic non-chiral case, it is well known that Roumeliotis, Kokkorakis, Kanellopoulos, and Fikioris have done excellent analyses of an electromagnetic cylindrical or spherical cavity with an internal off-axis small dielectric sphere [23–25]. The resonant frequency and Q-factor of cylindrical and spherical cavities containing chiral media have been examined by Rao, Xu, et al. [26, 27]. Additionally, chiral resonators have some potential applications in the design of novel bandpass filters [28].

In this study, the author pays attention to a perfectly conducting cylindrical and a spherical cavity loaded with a biisotropic chiral sphere, and these structures are evidently helpful to the measurement of constitutive parameters of chiral materials. In the following sections, two cases of magnetic and electric modes are treated carefully using a boundary-value approach, and the formulas for determining of the lower- and higher-order resonant frequency shifts are developed. Some numerical results are also presented to show some novel effect of chirality on the resonant frequency shift of different order modes.

2. GEOMETRY

Figs. 1(a)(b) present the geometries of the problem, in which one small biisotropic chiral sphere of radius R_1, is located at the point (ρ_0, φ_0, z_0) with respect to the cylindrical coordinate system $O_2(\rho_2, \varphi_2, z_2)$ in a perfectly conducting cylindrical cavity, and the point (d, θ_0, φ_0) in a perfectly conducting spherical cavity, respectively. The cavities are filled with non-chiral medium with permittivity ε_1 and permeability μ_1, and the radius of the cavities is R_2 and the height of cylindrical cavity is H. At first, the chiral sphere is supposed to be reciprocal and it is characterized by the permittivity ε, the permeability , μ and the chiral admittance ξ_c. For a time harmonic excitation $(e^{-i\omega t})$, its constitutive relations are assumed to be described by the following equations in an appropriate frequency range:

$$\vec{D} = \omega\vec{E} + i\xi_c\vec{B} \tag{1}$$

$$\vec{H} = i\xi_c\vec{E} + \vec{B}/\mu \tag{2}$$

where the three quantities ε, μ ,and ξ_c are all real numbers for the lossless case and complex if losses are considered.

3. FIELD EQUATIONS FOR THE CYLINDRICAL CAVITY

3.1 The Magnetic Mode Case (TE)

The corresponding unperturbed electric and magnetic fields in the case of magnetic mode (TE mode or H-mode) with respect to $O_2(\rho_2, \varphi_2, z_2)$ in cylindrical cavity are described by

$$\vec{E}_{mnl}(\rho_2, \varphi_2, z_2) = \vec{M}^{(1)}_{mnl}(\rho_2, \varphi_2, Z_2) \tag{3}$$

$$\vec{H}_{mnl}(\rho_2, \varphi_2, z_2) = -\frac{i}{\eta_1}\vec{N}^{(1)}_{mnl}(\rho_2, \varphi_2, z_2) \tag{4}$$

where $\eta = \sqrt{\frac{\mu_1}{\varepsilon_1}}, i = \sqrt{-1}$; $\vec{M}^{(1)}_{mnl}(\cdot)$ and $\vec{N}^{(1)}_{mnl}(\cdot)$ are the cylindrical vector wave functions of the first kind defined as follows:

$$\vec{M}^{(1)}_{mnl}(\rho_2, \varphi_2, z_2) = \Big[\frac{im}{\rho_2}J_m(k_{mn})\vec{e}_{\rho 2} - k_{mn}J'_m(k_{mn}\rho_2)\vec{e}_{\varphi 2}\Big]$$

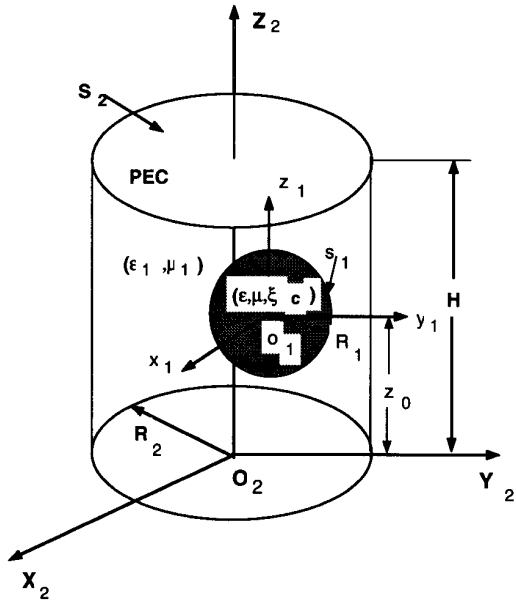

(a)

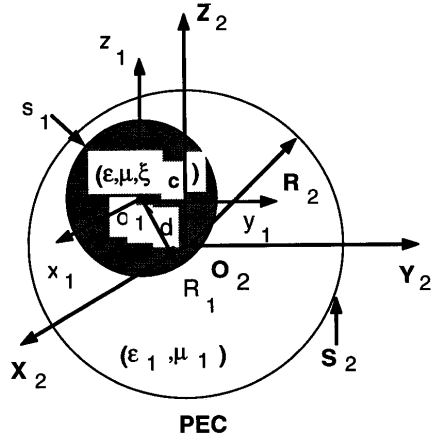

(b)

Figure 1. The geometries of the cylindrical and spherical cavities containing a biisotropic (non)reciprocal chiral sphere, respectively.

$$e^{im\varphi_2}\sin(k_z l z_2) \tag{5a}$$

$$\vec{N}^{(1)}_{mnl}(\rho_2,\varphi_2,z_2) = \frac{1}{k_{mnl}}\nabla\times\vec{M}^{(1)}_{mnl}(\rho_2,\varphi_2,z_2) \tag{5b}$$

with

$$k^2_{mnl} = k^2_{mn} + k^2_{zl}, \quad k_{zl} = l\pi/H, \quad l = 1,2,3,\cdots. \tag{5c}$$

in which J_m and J'_m stand for the Bessel function of the first kind and its derivative, respectively; while k_{mn} is determined by

$$J'_m(k_{mn}R_2) = 0, \quad n = 1,2,3,\cdots. \tag{6}$$

It is worth noting that, because of the smallness of chiral sphere, its scattered field is weak compared to the original field that can be regarded as the incident field of the chiral sphere, and furthermore it can be expressed as the following form by taking advantage of the translational addition theorem with respect to the spherical coordinate system $O(r,\theta,\varphi)$:

$$\vec{E}_{mnl} = \sum_{\mu=-\infty}^{\infty}\sum_{v=|\mu|}^{\infty}[A_{\mu-m,v}\vec{M}^{(1)}_{\mu v}(r,\theta,\varphi) + B_{\mu-m,v}\vec{N}^{(1)}_{\mu v}(r,\theta,\varphi)] \tag{7}$$

$$\vec{H}_{mnl} = -\frac{i}{\eta_1}\sum_{\mu=-\infty}^{\infty}\sum_{v=|\mu|}^{\infty}[A_{\mu-m,v}\vec{N}^{(1)}_{\mu v}(r,\theta,\varphi) + B_{\mu-m,v}\vec{M}^{(1)}_{\mu v}(r,\theta,\varphi)] \tag{8}$$

where $A_{\mu-m,v}$ and $B_{\mu-m,v}$ are shown in Appendix 1; $\vec{M}^{(1)}_{\mu v}(r,\theta,\varphi)$ and $\vec{N}^{(1)}_{\mu v}(r,\theta,\varphi)$ are the spherical vector wave functions, respectively. The electric and magnetic fields in the inner region of the chiral sphere ($r \le R_1$) are now expanded in terms of the generalized spherical vector wave functions as [29, 30]:

$$\vec{E}_I(r,\theta,\varphi) = \sum_{n'=1}^{\infty}\sum_{m'=-n'}^{n'}\Big[C_{m'n'}\vec{V}^{(1)}_{m'n'}(k_{mnl+},r,\theta,\varphi) + D_{m'n'}\vec{W}^{(1)}_{m'n'}(k_{mnl-},r,\theta,\varphi)\Big] \tag{9}$$

$$\vec{H}_I(r,\theta,\varphi) = -\frac{i}{\eta_c}\sum_{n'=1}^{\infty}\sum_{m'=-n'}^{n'}\Big[C_{m'n'}\vec{V}^{(1)}_{m'n'}(k_{mnl+},r,\theta,\varphi) - D_{m'n'}\vec{W}^{(1)}_{m'n'}(k_{mnl-},r,\theta,\varphi)\Big] \tag{10}$$

where $\eta_c = \sqrt{\frac{\mu}{\varepsilon+\mu\xi_c^2}}$ is the chiral admittance; k_{mnl+} and k_{mnl-} are the wavenumbers of the right- and left-handed circularly polarized eigenmodes in chiral sphere, and given by

$$k_{mnl\pm} = \frac{\pm\mu\xi_c + \sqrt{\mu\varepsilon + \mu^2\xi_c^2}}{\sqrt{\mu_1\varepsilon_1}} k_{mnl} \tag{11}$$

In (9) and (10), $\vec{V}^{(1)}_{m'n'}(\cdot)$ and $\vec{W}^{(1)}_{m'n'}(\cdot)$ are defined as

$$\begin{aligned}
&\left\{ \begin{array}{l} \vec{V}^{(1)}_{m'n'}(k_{mnl+}, r, \theta, \varphi) \\ \vec{W}^{(1)}_{m'n'}(k_{mnl-}, r, \theta, \varphi) \end{array} \right\} \\
&= \frac{1}{\sqrt{2}}\left[\vec{M}^{(1)}_{m'n'}(k_{mnl\pm}, r, \theta, \varphi) \pm \vec{N}^{(1)}_{m'n'}(k_{mnl\pm}, r, \theta, \varphi)\right] \\
&= \frac{e^{im'\varphi}}{\sqrt{2}} \left\{ \pm \frac{1}{k_{mnl\pm} r} j_{n'}(k_{mnl\pm} r) n'(n'+1) P^{m'}_{n'}(\cos\theta)\vec{e}_r \right. \\
&+ j_{n'}(k_{mnl\pm} r)\left[i\tau_{m'n'}\vec{e}_\theta - \pi_{m'n'}(\theta)\vec{e}_\varphi \right] \\
&\left. \pm \frac{1}{k_{mnl\pm} r} \frac{\partial}{\partial r}[r j_{n'}(k_{mnl\pm} r)](\pi_{m'n'}(\theta)\vec{e}_\theta + i\tau_{m'n'}(\theta)\vec{e}_\varphi) \right\}
\end{aligned} \tag{12a, b}$$

In $(12a, b)$, $j_{n'}$ is the spherical Bessel function of the first kind; $\pi_{m'n'}(\theta) = \frac{\partial}{\partial\theta} P^{m'}_{n'}(\cos\theta), \tau_{m'n'}(\theta) = \frac{m'}{\sin\theta} P^{m'}_{n'}(\cos\theta), P^{m'}_{n'}(\cos\theta)$ is the associated Legendre function; $\vec{e}_r, \vec{e}_\theta$ and $\vec{e}_\varphi$ are three unit vectors of the coordinate system $O_1(r, \theta, \varphi)$, see Fig. 1. The scattered fields of chiral sphere are written as

$$\begin{aligned}
\vec{E}_s = \sum_{n'=1}^{\infty} \sum_{m'=-n'}^{n'} \Big[& E_{m'n'} \vec{V}^{(3)}_{m'n'}(k_{mnl}, r, \theta, \varphi) \\
& + F_{m'n'} \vec{W}^{(3)}_{m'n'}(k_{mnl}, r, \theta, \varphi) \Big]
\end{aligned} \tag{13}$$

$$\begin{aligned}
\vec{H}_s = -\frac{i}{\eta_1} \sum_{n'=1}^{\infty} \sum_{m'=-n'}^{n'} \Big[& E_{m'n'} \vec{V}^{(3)}_{m'n'}(k_{mnl}, r, \theta, \varphi) \\
& - F_{m'n'} \vec{W}^{(3)}_{m'n'}(k_{mnl}, r, \theta, \varphi) \Big]
\end{aligned} \tag{14}$$

where $\vec{V}^{(3)}_{m'n'}(\cdot)$ and $\vec{W}^{(3)}_{m'n'}(\cdot)$ are the generalized spherical vector wave functions of the third kind and their expressions are given by $(12a, b)$

in which $k_{mnl\pm}$ should be replaced by k_{mnl}, and $j_{n'}$ replaced by the special Hankel function of the first kind $h_{n'}^{(1)}$, respectively. Here $E_{m'n'}, F_{m'n'}$ together with $C_{m'n'}, D_{m'n'}$ are unknown mode expanding coefficients. Straightforwardly, applying boundary conditions at the chiral sphere surface yields four sets of equations:

$$\begin{vmatrix} j_{n'+} & j_{n'-} & -h_{n'} & -h_{n'} \\ \partial j_{n'+} & -\partial j_{n'-} & -\partial h_{n'} & \partial h_{n'} \\ \eta j_{n'+} & -\eta j_{n'-} & -h_{n'} & h_{n'} \\ \eta\partial j_{n'+} & \eta\partial j_{n'-} & -\partial h_{n'} & -\partial h_{n'} \end{vmatrix} \begin{vmatrix} C_{m'n'} \\ D_{m'n'} \\ E_{m'n'} \\ F_{m'n'} \end{vmatrix} = \sqrt{2} \begin{vmatrix} A_{m'-m,n'} j_{n'} \\ B_{m'-m,n'} \partial j_{n'} \\ B_{m'-m,n'} j_{n'} \\ A_{m'-m,n'} \partial j_{n'} \end{vmatrix} \tag{15}$$

where

$$j_{n'} = j_{n'}(k_{mnl}R_1), h_{n'} = h_{n'}^{(1)}(k_{mnl}R_1), \partial j_{n'} = \frac{d}{rdr}(rj_{n'}(r))|_{r=k_{mnl}R_1}$$
$$\partial h_{n'} = \frac{d}{rdr}(rh_{n'}^{(1)}(r))|_{r=k_{mnl}R_1}, j_{n'\pm} = j_{n'}(k_{mnl\pm}R_1)$$
$$\partial j_{n'\pm} = \frac{d}{r_\pm dr_\pm}(r_\pm j_{n'}(r_\pm))|_{r_\pm=k_{mnl\pm}R_1},$$
$$\partial h_{n'\pm} = \frac{d}{r_\pm dr_\pm}(r_\pm h_{n'}^{(1)}(r_\pm))|_{r=k_{mnl\pm}R_1}, \eta = \eta_1/\eta_c$$

Some algebraic manipulation from (15) leads to the following expressions,

$$E_{m'n'} = \sqrt{2}(A_{m'-m,n'} D_{1n'} + B_{m'-m,n'} D_{2n'}) \tag{16}$$
$$F_{m'n'} = \sqrt{2}(A_{m'-m,n'} D_{3n'} + B_{m'-m,n'} D_{4n'}) \tag{17}$$

and the coefficients $D_{1n'}, \cdots, D_{4n'}$ are shown in Appendix 2. In the region $V_A \in (\varepsilon_1, \mu_1)$ the total fields are also governed by vector Helmholtz equation with corresponding wavenumber $K_{mnl}^{(t)}$, i.e.,

$$\nabla^2(\vec{F}_{mnl} + \vec{F}_s) + K_{mnl}^{(t)}(\vec{F}_{mnl} + \vec{F}_s) = 0 \tag{18}$$

where $F = E, H$, and using the vector Green's function as Roumeliotis, et al. have done, the relative resonant frequency can be derived, i.e.,

$$\frac{\Delta f_{mnl}}{f_{mnl}} = -\frac{\sum_{i=1}^{N} \Delta f_{mnl}^{(i)}}{f_{mnl}} = \frac{I_1}{2k_{mnl}^2 I_2} \tag{19}$$

where $\Delta f_{mnl}^{(i)}$ is the ith-order perturbed resonant frequency shift, and the perturbed factor I_1, is calculated by

$$I_1 = \oiint [(\vec{e}_r \times \vec{E}_{mnl}^t) \cdot (\nabla \times \vec{E}_{mnl}^*) - (\nabla \times \vec{E}_{mnl}^t) \cdot (\vec{e}_r \times \vec{E}_{mnl}^*)] ds_1 \tag{20a}$$

$$I_2 = \iiint_{v_2} |\vec{E}_{mnl}|^2 dv_2 = \frac{\pi H}{2} \left((k_{mn} R_2)^2 - m^2 \right) J_m^2 (k_{mn} R_2) \tag{20b}$$

here v_2 is the total space of the cavity, and the boundary conditions for perfectly conducting walls of cylindrical cavity in (20a) and small electric size of chiral sphere in (20b) have been taken into account. Substituting (7), (8), (13) and (14) into (20a) combined with the orthogonal properties of generalized spherical vector wave functions, we get the following expression after some mathematical manipulations,

$$\begin{aligned} I_1 = k_{mnl} R_1^2 \int_0^{\pi} \int_0^{2\pi} & \left\{ \left\{ \sum_{\mu=-\infty}^{\infty} \sum_{v=|\mu|}^{\infty} S_v (A_{\mu-m,v}^* \partial j_v \vec{B}_{\mu v}^* + \vec{B}_{\mu-m,v}^* j_v \vec{C}_{\mu v}^*) \right\} \right. \\ & \cdot \left\{ \sum_{n'=1}^{\infty} \sum_{m'=-n'}^{n'} S_{n'} (G_{m'n'} h_{n'} \vec{B}_{m'n'} - H_{m'n'} \partial h_{n'} \vec{C}_{m'n'}) \right\} \\ & - \left\{ \sum_{n'=1}^{\infty} \sum_{m'=-n'}^{n'} S_{n'} (G_{m'n'} \partial h_{n'} \vec{B}_{m'n'} + H_{m'n'} h_{n'} \vec{C}_{m'n'}) \right\} \\ & \left. \cdot \left\{ \sum_{\mu=-\infty}^{\infty} \sum_{v=|\mu|}^{\infty} S_v (A_{\mu-m,v}^* j_v \vec{B}_{\mu v}^* - \vec{B}_{\mu-m,v}^* \partial j_v \vec{C}_{\mu v}^*) \right\} \right\} \sin\theta_1 d\theta_1 d\varphi_1 \end{aligned} \tag{21}$$

where $S_x = \sqrt{x(x+1)}, x = v, n'$; $\vec{B}_{\mu v(m'n')}$ and $\vec{C}_{\mu v(m'n')}$ are the complex spherical surface vector functions, given by

$$\vec{B}_{\mu v} = \frac{e^{i\mu\varphi}}{S_v} \left[\frac{\partial P_v^{\mu}(\cos\theta)}{\partial\theta} \vec{e}_{\theta} + \frac{i\mu}{\sin\theta} P_v^{\mu}(\cos\theta) \vec{e}_{\varphi} \right] \tag{22}$$

$$\vec{C}_{\mu v} = \frac{e^{i\mu\varphi}}{S_v} \left[-\frac{\partial P_v^{\mu}(\cos\theta)}{\partial\theta} \vec{e}_{\varphi} + \frac{i\mu}{\sin\theta} P_v^{\mu}(\cos\theta) \vec{e}_{\theta} \right] \tag{23}$$

and $G_{m'n'} = (E_{m'n'} + F_{m'n'})/\sqrt{2}$, $H_{m'n'} = (E_{m'n'} - F_{m'n'})/\sqrt{2}$. Alternatively, the perturbed factor I_1 can be decoupled into

$$I_1 = \sum_{j=1}^{N} I_1^{(j)} \tag{24}$$

where $I_1^{(j)}$ $(j = 1, ..., N)$ is the j th-order perturbed factor, expressed by

$$\begin{aligned} I_1^{(j)} = -\frac{j(j+1)i}{k_{mnl}} \int_0^{\pi} \int_0^{2\pi} \Bigg\{ & D_{1j+3j} \sum_{\mu=-j}^{j} |A_{-\mu-m,j}|^2 |\vec{B}_{\mu j}|^2 \\ & + D_{2j-4j} \sum_{\mu=-j}^{j} |B_{-\mu-m,j}|^2 |\vec{C}_{\mu j}|^2 \Bigg\} \sin\theta d\theta d\varphi \end{aligned} \tag{25}$$

where $D_{1j\pm3j} = D_{1j} \pm D_{3j}$, $D_{2j\pm4j} = D_{2j} \pm D_{4j}$; $D_{1j-3j} = D_{2j+4j}$ and the approximate formulas of (A3) are introduced above.

Finally, using the orthogonal relations of $\vec{B}_{\mu v}$ and $\vec{C}_{\mu v}$ in Appendix 3 and in [23], we obtain the analytical formulas for the first-, second-, and third-perturbed relative resonant frequency shifts as follow:

$$\Delta\tilde{f}^{(1)} = 2C[\tilde{D}_{11+31}(B_{m\pm1}C_zC_\alpha + B_mS_zS_\alpha) + \tilde{D}_{21-41}B_{m\pm1}S_z] \tag{26}$$

and

$$\begin{aligned} & C = \frac{k_{mn}^2 R_1^3}{H[(k_{mn}R_2)^2 - m^2]J_m^2(k_{mn}R_2)}, \quad S(C)_\alpha = \left(\frac{k_{mn(zl)}}{k_{mnl}}\right)^2 \\ & C_z = \cos^2(k_{zl}z_0), \quad S_z = \sin^2(k_{zl}z_0), \\ & B_{m\pm q} = J_{m+q}^2(k_{mn}\rho_0) + J_{m-q}^2(k_{mn}\rho_0) \end{aligned}$$

$$\begin{aligned} \Delta\tilde{f}^{(2)} = {} & \frac{CX^2}{3} \cdot \Big\{ \tilde{D}_{12+32}[B_{m\pm2}C_zS_\alpha C_\alpha + B_{m\pm1}S_z(C_\alpha - S_\alpha)^2 \\ & + 3B_mC_zC_\alpha S_\alpha] + \tilde{D}_{22-42}(B_{m\pm2}S_zS_\alpha + B_{m\pm1}C_zC_\alpha) \Big\} \end{aligned} \tag{27}$$

$$\begin{aligned} \Delta\tilde{f}^{(3)} = {} & \frac{CX^4}{75} \cdot \Big\{ \tilde{D}_{13+33}[\frac{5}{4}B_{m\pm3}C_zC_\alpha S_\alpha^2 + \frac{10}{3}B_{m\pm2}S_zS_\alpha(\frac{3}{2}S_\alpha - 1)^2 \\ & + \frac{1}{12}B_{m\pm1}C_zC_\alpha(15C_\alpha - 11)^2 + \frac{1}{2}B_mS_zS_\alpha(1 - 5C_\alpha)^2] \\ & + \tilde{D}_{23-43}[\frac{1}{12}B_{m\pm1}S_z(1 - 5C_\alpha)^2 + \frac{10}{3}B_{m\pm2}C_zC_\alpha S_\alpha + \frac{5}{4}B_{m\pm3}S_zS_\alpha^2] \Big\} \end{aligned} \tag{28}$$

and $\Delta\tilde{f}^{(p)} = \frac{\Delta f_{mnl}^{(p)}}{f_{mnl}}$, $p = 1, 2, 3$; $X = k_{mnl}R_1$,

$$\tilde{D}_{1n+3n} = \frac{[n(\varepsilon + \mu\xi_c^2) + (n+1)\varepsilon_1]\mu_1 - [n\varepsilon + (n+1)\varepsilon_1]\mu}{n[n\varepsilon + (n+1)\varepsilon_1]\mu + (n+1)[n(\varepsilon + \mu\xi_c^2) + (n+1)\varepsilon_1]\mu_1} \tag{29a}$$

$$\tilde{D}_{2n-4n} = \frac{n(\varepsilon_1 - \varepsilon)\mu + (n+1)[\varepsilon_1 - (\varepsilon + \mu\xi_c^2)]\mu_1}{n[n\varepsilon + (n+1)\varepsilon_1]\mu + (n+1)[n(\varepsilon + \mu\xi_c^2) + (n+1)\varepsilon_1]\mu_1} \tag{29b}$$

The total resonant frequency shift is calculated by

$$\Delta f_{mnl} = \Delta f_{mnl}^{(1)} + \Delta f_{mnl}^{(2)} + \Delta f_{mnl}^{(3)} + O(R_{12}^9) \tag{30}$$

where $R_{12} = R_1/R_2$. Here the higher-order perturbation corresponds to the contribution of higher-order polarisability moment of chiral sample. Comparing our results with the traditional perturbation formula under the condition of Rayleigh approximation for non-chiral materials [25], it is exact enough here to determine the resonant frequency shift of an perfectly conducting cylindrical cavity loaded with reciprocal chiral sphere. Since the higher-order resonant frequency shift is taken into account, the restriction on the dimension of chiral sphere is relaxed greatly and only if the chiral sphere is kept away from the cavity walls. Additionally, it is interesting to note that, for non-magnetic chiral sphere ($\mu_1 = \mu$), (29) is turned into:

$$\tilde{D}_{1n+3n} = \frac{n\mu\xi_c^2}{n[n\varepsilon + (n+1)\varepsilon_1] + (n+1)[n(\varepsilon + \mu\xi_c^2) + (n+1)\varepsilon_1]} > 0 \tag{31a}$$

$$\tilde{D}_{2n-4n} = -\frac{\varepsilon - \varepsilon_1 + (n+1)\mu\xi_c^2}{n[n\varepsilon + (n+1)\varepsilon_1] + (n+1)[n(\varepsilon + \mu\xi_c^2) + (n+1)\varepsilon_1]} < 0 \tag{31b}$$

and especially, for non-chiral sphere, (29) reduces to the most simple form:

$$\tilde{D}_{1n+3n} = \frac{\mu_1 - \mu}{n\mu + (n+1)\mu_1} \tag{32a}$$

$$\tilde{D}_{2n-4n} = \frac{\varepsilon_1 - \varepsilon}{n\varepsilon + (n+1)\varepsilon_1} \tag{32b}$$

3.2. The Electric Mode Case (TM)

The unperturbed electric and magnetic fields for electric mode (TM) in a perfectly conducting cylindrical cavity are

$$\vec{E}_{mnl}(\rho_2,\varphi_2,z_2) = i\eta_1 \vec{N}^{(1)}_{mnl}(\rho_2,\varphi_2,z_2) \tag{33}$$

$$\vec{H}_{mnl}(\rho_2,\varphi_2,z_2) = \vec{M}^{(1)}_{mnl}(\rho_2,\varphi_2,z_2) \tag{34}$$

and in $O_1(r,\theta,\varphi)$,

$$\vec{E}_{mnl} = i\eta_1 \sum_{\mu=-\infty}^{\infty}\sum_{v=|\mu|}^{\infty}\left[A'_{\mu-m,v}\vec{N}^{(1)}_{\mu v}(r,\theta,\varphi) + B'_{\mu-m,v}\vec{M}^{(1)}_{\mu v}(r,\theta,\varphi)\right] \tag{35}$$

$$\vec{H}_{mnl} = \sum_{\mu=-\infty}^{\infty}\sum_{v=|\mu|}^{\infty}\left[A'_{\mu-m,v}\vec{M}^{(1)}_{\mu v}(r,\theta,\varphi) + B'_{\mu-m,v}\vec{N}^{(1)}_{\mu v}(r,\theta,\varphi)\right] \tag{36}$$

where $A'_{\mu-m,v}$ and $B'_{\mu-m,v}$ are also given in Appendix 1. The internal and scattered fields of the reciprocal chiral sphere can be described by

$$\vec{E}_I(r,\theta,\varphi) = i\eta_c \sum_{n'=1}^{\infty}\sum_{m'=-n'}^{n'}\Big[c_{m'n'}\vec{V}^{(1)}_{m'n'}(k'_{mnl+},r,\theta,\varphi) - d_{m'n'}\vec{W}^{(1)}_{m'n'}(k'_{mnl-},r,\theta,\varphi)\Big] \tag{37}$$

$$\vec{H}_I(r,\theta,\varphi) = \sum_{n'=1}^{\infty}\sum_{m'=-n'}^{n'}\Big[c_{m'n'}\vec{V}^{(1)}_{m'n'}(k'_{mnl+},r,\theta,\varphi) + d_{m'n'}\vec{W}^{(1)}_{m'n'}(k'_{mnl-},r,\theta,\varphi)\Big] \tag{38}$$

$$\vec{E}_s = i\eta_1 \sum_{n'=1}^{\infty}\sum_{m'=-n'}^{n'}\Big[e_{m'n'}\vec{V}^{(3)}_{m'n'}(k'_{mnl},r,\theta,\varphi) - f_{m'n'}\vec{W}^{(3)}_{m'n'}(k'_{mnl},r,\theta,\varphi)\Big] \tag{39}$$

$$\vec{H}_s = \sum_{n'=1}^{\infty}\sum_{m'=-n'}^{n'}\Big[e_{m'n'}\vec{V}^{(3)}_{m'n'}(k'_{mnl},r,\theta,\varphi) + f_{m'n'}\vec{W}^{(3)}_{m'n'}(k'_{mnl},r,\theta,\varphi)\Big] \tag{40}$$

with

$$k'_{mnl\pm} = \frac{\pm\mu\xi_c + \sqrt{\mu\varepsilon + \mu^2\xi_c^2}}{\sqrt{\mu_1\varepsilon_1}} k'_{mnl}, \tag{41}$$

$$k'_{mnl}{}^2 = k'_{mn}{}^2 + k'_{zl}{}^2, \qquad k'_{zl} = l\pi/H, l = 1, 2, 3, \cdots, \tag{42}$$

$$J_m(k'_{mn}R_2) = 0, \qquad n = 0, 1, 2, 3, \cdots. \tag{43}$$

and the above unknown coefficients are determined by

$$[D] \begin{bmatrix} c_{m'n'} \\ d_{m'n'} \\ e_{m'n'} \\ f_{m'n'} \end{bmatrix} = \sqrt{2} \begin{bmatrix} A'_{m'-m,n'} j_{n'} \\ B'_{m'-m,n'} \partial j_{n'} \\ B'_{m'-m,n'} j_{n'} \\ A'_{m'-m,n'} \partial j_{n'} \end{bmatrix} \tag{44}$$

or

$$e_{m'n'} = \sqrt{2}(A'_{m'-m,n'} d_{1n'} + B'_{m'-m,n'} d_{2n'}) \tag{45}$$

$$f_{m'n'} = \sqrt{2}(A'_{m'-m,n'} d_{3n'} + B'_{m'-m,n'} d_{4n'}) \tag{46}$$

where the coefficient matrix $[D]$ takes the same form as in (15) but here $\eta = \eta_c/\eta_1$,, and the tedious expressions $d_{1n'}, \cdots,$ and $d_{4n'}$ can refer to Appendix 2. Correspondingly, the perturbed factor I_1 in (20) here becomes

$$\begin{aligned} I_1 = {} & k'_{mnl} R_1^2 \int_0^{\pi} \int_0^{2\pi} \\ & \left\{ \left\{ \sum_{\mu=-\infty}^{\infty} \sum_{v=|\mu|}^{\infty} S_v (A'^*_{\mu-m,v} \partial j_v \vec{B}^*_{\mu v} + \vec{B}'^*_{\mu-m,v} j_v \vec{C}^*_{\mu v}) \right\} \right. \\ & \cdot \left\{ \sum_{n'=1}^{\infty} \sum_{m'=-n'}^{n'} S_{n'} (g_{m'n'} h_{n'} \vec{B}_{m'n'} - h_{m'n'} \partial h_{n'} \vec{C}_{m'n'}) \right\} \\ & - \left\{ \sum_{n'=1}^{\infty} \sum_{m'=-n'}^{n'} S_{n'} (g_{m'n'} \partial h_{n'} \vec{B}_{m'n'} + h_{m'n'} h_{n'} \vec{C}_{m'n'}) \right\} \\ & \left. \cdot \left\{ \sum_{\mu=-\infty}^{\infty} \sum_{v=|\mu|}^{\infty} S_v (A'^*_{\mu-m,v} j_v \vec{B}^*_{\mu v} - \vec{B}'^*_{\mu-m,v} \partial j_v \vec{C}^*_{\mu v}) \right\} \right\} \sin\theta_1 d\theta_1 d\varphi_1 \end{aligned} \tag{47}$$

and

$$I_2 = \frac{\pi H}{\delta_{l0}}(k'_{mn}R_2)^2 J^2_{m+1}(k'_{mn}R_2) \tag{48}$$

where $\delta_{l0} = \begin{cases} 1, & l=0 \\ 2, & l\neq 0 \end{cases}$, $g_{m'n'} = (e_{m'n'} + f_{m'n'})/\sqrt{2}$, $h_{m'n'} = (e_{m'n'} - f_{m'n'})/\sqrt{2}$. As the case stands, the j th-order perturbed factor takes the following form,

$$\begin{aligned} I_1^{(j)} = -i\frac{j(j+1)}{k'_{mnl}} \int_0^{\pi}\int_0^{2\pi} \Bigg\{ & D_{2j-4j} \sum_{\mu=-j}^{j} |A'_{-\mu-m,j}|^2 |\vec{B}_{\mu j}|^2 \\ & + D_{1j+3j} \sum_{\mu=-j}^{j} |B'_{-\mu-m,j}|^2 |\vec{C}_{\mu j}|^2 \Bigg\} \sin\theta d\theta d\varphi \end{aligned} \tag{49}$$

Also, the first-, second-, and third- perturbed relative resonant frequency shifts can be derived after some mathematical manipulations, given by

$$\Delta\tilde{f}^{(1)'} = C'[\tilde{D}_{21-41}(B'_{m\pm1}S'_zC'_\alpha + B'_mC'_zS'_\alpha) + \tilde{D}_{11+31}B'_{m\pm1}C'_z] \tag{50}$$

and

$$\begin{aligned} & C' = \frac{\delta_{l0}R_1^3}{HR_2^2J^2_{m+1}(k'_{mn}R_2)}, \quad S'(C')_\alpha = (\frac{k'_{mn(zl)}}{k'_{mnl}})^2 \\ & C'_z = \cos^2(k'_{zl}z_0), \quad S'_z = \sin^2(k'_{zl}z_0), \\ & B'_{m\pm q} = J^2_{m+q}(k'_{mn}\rho_0) + J^2_{m-q}(k'_{mn}\rho_0) \end{aligned}$$

$$\begin{aligned} \Delta\tilde{f}^{(2)'} = \frac{C'X'^2}{6} \Big\{ & \tilde{D}_{22-42}[B_{m\pm2}S'_zS'_\alpha C'_\alpha + B'_{m\pm1}C'_z(C'_\alpha - S'_\alpha)^2 \\ & + 3B'_mS'_zC'_\alpha S'_\alpha] + \tilde{D}_{12+32}(B'_{m\pm2}C'_zS'_\alpha + B'_{m\pm1}S'_zC'_\alpha) \Big\} \end{aligned} \tag{51}$$

4. THE CASE OF SPHERICAL CAVITY

In Fig. 1 (b), when the biisotropic reciprocal chiral sphere is placed in a perfectly conducting spherical cavity, the corresponding unperturbed

electric and magnetic fields for TE-mode in the spherical coordinate system $O_2(r_2, \theta_2, \varphi_2)$ are written as

$$\vec{E}_{mn}(r_2, \theta_2, \varphi_2) = \vec{M}^{(1)}_{mn}(r_2, \theta_2, \varphi_2) \tag{57}$$

$$\vec{H}_{mn}(r_2, \theta_2, \varphi_2) = -\frac{i}{\eta_1}\vec{N}^{(1)}_{mn}(r_2, \theta_2, \varphi_2) \tag{58}$$

where $\vec{M}^{(1)}_{mn}(\cdot)$ and $\vec{N}^{(1)}_{mn}(\cdot)$ are the spherical vector wave functions of the first kind with wavenumber k_{nl} determined by

$$j_n(k_{nl}R_2) = 0, \quad n, l = 1, 2, 3, \cdots. \tag{59}$$

and $j_n(k_{nl}R_2)$ is the spherical Bessel function of the first kind. Furthermore, (57) and (58) can be expressed as the following form by taking advantage of the translational addition theorem with respect to the spherical coordinate system $O_1(r, \theta, \varphi)$

$$\vec{E}_{mn} = \sum_{v=1}^{\infty}\sum_{\mu=-v}^{v}\left[A^{mn}_{\mu v}\vec{M}^{(1)}_{\mu v}(r, \theta, \varphi) + B^{mn}_{\mu v}\vec{N}^{(1)}_{\mu v}(r, \theta, \varphi)\right] \tag{60}$$

$$\vec{H}_{mn} = -\frac{i}{\eta_1}\sum_{v=1}^{\infty}\sum_{\mu=-v}^{v}\left[A^{mn}_{\mu v}\vec{N}^{(1)}_{\mu v}(r, \theta, \varphi) + B^{mn}_{\mu v}\vec{M}^{(1)}_{\mu v}(r, \theta, \varphi)\right] \tag{61}$$

where $A^{mn}_{\mu v}$ and $B^{mn}_{\mu v}$ are shown in [25, 31]. Then, following an analogous way adopted from (9) to (25) and using the substitutions:

$$k_{nl} \Rightarrow k_{mnl},\ k_{nl\pm} \Rightarrow k_{mnl\pm},\ A(B)^{mn}_{\mu v} \Rightarrow A(B)_{\mu-m,v} \tag{62}$$

we can obtain arbitrary order resonant frequency shift for TE$_{mnl}$ mode:

$$\begin{aligned}\Delta\tilde{f}^{(1)} &= \frac{2}{9}N_0[\tilde{D}_{11+31}(|A^{mn}_{-11}|^2 + 2|A^{mn}_{01}|^2 + 4|A^{mn}_{11}|^2) \\ &\quad + \tilde{D}_{21-41}(|B^{mn}_{-11}|^2 + 2|B^{mn}_{01}|^2 + 4|B^{mn}_{11}|^2)] \\ \Delta\tilde{f}^{(2)} &= \frac{1}{50}N_0X^2 \cdot [\tilde{D}_{12+32}(\frac{1}{6}|A^{mn}_{-22}|^2 + \frac{2}{3}|A^{mn}_{-12}|^2 \\ &\quad + 4|A^{mn}_{02}|^2) + 24|A^{mn}_{12}|^2) + 96|A^{mn}_{22}|^2)\end{aligned} \tag{63}$$

$$+\tilde{D}_{22-42}(\frac{1}{6}|B^{mn}_{-22}|^2+\frac{2}{3}|B^{mn}_{-12}|^2$$
$$+4|B^{mn}_{02}|^2)+24|B^{mn}_{12}|^2)+96|B^{mn}_{22}|^2)] \quad (64)$$

$$\Delta\tilde{f}^{(3)}=\frac{4}{3675}N_0X^4\cdot[\tilde{D}_{13+33}(\frac{1}{180}|A^{mn}_{-33}|^2+\frac{1}{30}|A^{mn}_{-23}|^2+\frac{1}{3}|A^{mn}_{-13}|^2$$
$$+4|A^{mn}_{03}|^2)+48|A^{mn}_{13}|^2)+480|A^{mn}_{23}|^2+2880|A^{mn}_{33}|^2)$$
$$+\tilde{D}_{23-43}(\frac{1}{180}|B^{mn}_{-33}|^2+\frac{1}{30}|B^{mn}_{-23}|^2+\frac{1}{3}|B^{mn}_{-13}|^2$$
$$+4|B^{mn}_{03}|^2)+48|B^{mn}_{13}|^2)+480|A^{mn}_{23}|^2+2880|B^{mn}_{33}|^2)] \quad (65)$$

with $\Delta\tilde{f}^{(p)}=\frac{\Delta f^{(p)}_{nl}}{f_{mnl}}$, $N_0=\frac{R^3_{12}}{j^2_{n+1}(k_{nl}R_2)}\frac{(2n+1)}{n(n+1)}\frac{(n-m)!}{(n+m)!}$, $X=k_{nl}R_1$. So the total resonant frequency shift is determined by (30). As a special case, in Fig. 1(b), when the chiral sphere is located at the center of spherical cavity, since

$$\lim_{d\to 0}A^{mn}_{\mu v}=\delta_{m\mu}\delta_{nv},\ \lim_{d\to 0}B^{mn}_{\mu v}=0 \quad (66)$$

we find,

$$\frac{\Delta f_{m1l}}{f_{1l}}=\frac{2}{3}\frac{1}{j^2_2(k_{1l}R_2)}R^3_{12}\tilde{D}_{11+31} \quad (67)$$

$$\frac{\Delta f_{m2l}}{f_{2l}}=\frac{1}{15}\frac{(k_{2l}R_2)^2}{j^2_3(k_{2l}R_2)}R^5_{12}\tilde{D}_{12+32} \quad (68)$$

$$\frac{\Delta f_{m3l}}{f_{3l}}=\frac{4}{1575}\frac{(k_{3l}R_2)^4}{j^2_4(k_{3l}R_2)}R^7_{12}\tilde{D}_{13+33} \quad (69)$$

and generally $(n\geq 1)$,

$$\frac{\Delta f_{mnl}}{f_{nl}}=\frac{n+1}{(1\cdot 3\cdot 5\cdots(2n-1))^2(2n+1)}\frac{(k_{nl}R_2)^{2(n-1)}}{j^2_{n+1}(k_{nl}R_2)}R^{2n+1}_{12}\tilde{D}_{1n+3n} \quad (70)$$

It is noting that, only n th-order perturbation has contribution to the resonant frequency shift of TE$_{mnl}$ mode. On the other hand, similar results can be obtained for TM$_{mnl}$ mode and are suppressed here.

In the strict sense, the above formulas are only suited for the three-parameter reciprocal chiral material. However, we can easily extend our results to biisotropic four-parameter nonreciprocal chiral case. It

is known that the constitutive behaviour of biisotropic nonreciprocal chiral medium can be described by the following equations [32–38],

$$\vec{D} = \varepsilon\vec{E} + (\chi + i\kappa)\vec{H} \tag{71}$$

$$\vec{B} = \mu\vec{H} + (\chi - i\kappa)\vec{E} \tag{72}$$

where χ is the nonreciprocity parameter, and κ the chirality parameter. Physically, only if $\chi = 0$ (71) and (71) are equivalent to (1) and (2). When the loaded chiral sphere in Fig.1 is nonreciprocal, the arbitrary order frequency shift for both TE_{mnl} and TM_{mnl} modes in cylindrical or spherical cavity can be calculated according to the formulas developed in above sections by using the following substitutions for $\tilde{D}_{1n+3n}$ and $\tilde{D}_{2n-4n}$:

$$\tilde{D}_{1n+3n} = \frac{[n\varepsilon + (n+1)\varepsilon_1](\mu_1 - \mu) + n(\chi^2 + \kappa^2)}{[n\varepsilon + (n+1)\varepsilon_1][n\mu + (n+1)\mu_1] - n^2(\chi^2 + \kappa^2)} \tag{73}$$

$$\tilde{D}_{2n-4n} = \frac{[n\mu + (n+1)\mu_1](\varepsilon_1 - \varepsilon) + n(\chi^2 + \kappa^2)}{[n\varepsilon + (n+1)\varepsilon_1][n\mu + (n+1)\mu_1] - n^2(\chi^2 + \kappa^2)} \tag{74}$$

where $n = 1, 2, \cdots, N$; and here the contribution of higher-order polarisability moment of nonreciprocal chiral sample to the higher-order resonant frequency shift is also considered. In (73) and (74), $\kappa = 0$ is the nonactive case. Obviously, the nonreciprocity parameter χ has similar effect as κ on the resonant frequency shift of TE_{mnl} and TM_{mnl} modes.

5. NUMERICAL RESULTS AND REMARKS

To validate the analytical model, this section presents the calculated values of lower- and higher-relative resonant frequency shifts in a cylindrical cavity to demonstrate the influences of geometrical size as well as constitutive parameters of chiral sphere. As have been pointed out [5–15], the chiral samples can be fabricated by embedding identical, randomly oriented chiral inclusions in a continuous material. All the parameters chosen here for calculations are in a realizable range and related to some publications. The loss of chiral sphere is neglected here so that the attenuation by chiral sphere can not mask effects produced by chirality. For practical consideration, the permittivity ε_1, and permeability μ_1, are chosen to be $\varepsilon_1 = \varepsilon_0$, $\mu_1 = \mu_0$ and the eigenvalues $k_{mn}R_2(k'_{mn}R_2)$ of the empty cylindrical cavity are given

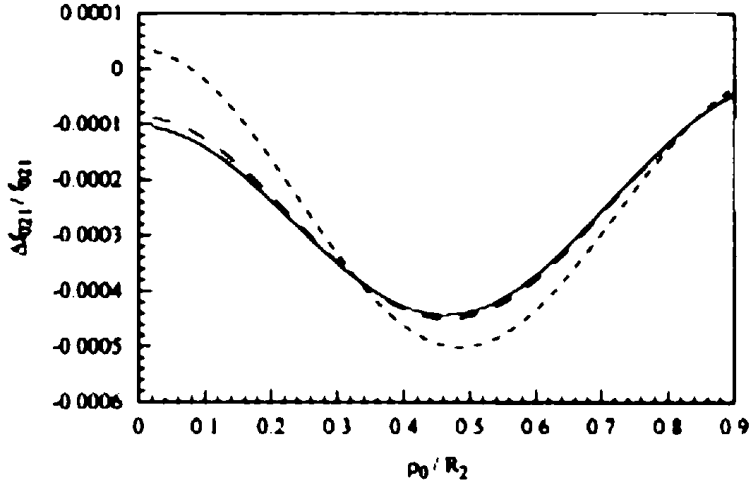

Figure 2. $\frac{\Delta f_{021}}{f_{021}}$ versus ρ_0/R_2 in a perfectly conducting cylindrical cavity with a chiral sphere: $R_1/R_2 = 0.05$, $R_2/H_2 = 1.0$, $z_0/H = 0.6$, $\varepsilon = 3.5\varepsilon_0$, $\mu = 1.2\mu_0$, $\xi_c = 0$ (——); $10^{-3}\Omega^{-1}$ (– – –); $3 \times 10^{-3}\Omega^{-1}$ (- - - -).

by: $k_{02}R_2 = 3.83171$, $k_{11}R_2 = 1.84118$, $k_{12}R_2 = 5.33144$, $k_{21}R_2 = 3.05424$, $k_{22}R_2 = 6.70613$; $k'_{01}R_2 = 2.404825$, $k'_{11}R_2 = 3.83171$.

At first, Fig. 2 depicts $\frac{\Delta f_{021}}{f_{021}}$ versus ρ_0/R_2 corresponding to different chiral admittances.

The results are obtained using the first-order perturbed formula (26), and are also checked by taking account of the contributions of higher-order resonant frequency shifts (27–29). Since $R_1/R_2 = 0.05 \ll 1$ the computed data show excellent agreement with (26) that can predict the perturbation effect of chiral sphere exactly.

In Fig. 2, $\xi_c = 0$ is the non-chiral case. Notice that, because of $\varepsilon > \varepsilon_1(\varepsilon_1 = \varepsilon_0)$ and $\mu > \mu_1(\mu_1 = \mu_0)$ the total resonant frequency keeps $\Delta f_{mnl} < 0$ for non-chiral sphere. Such case is also suitable for chiral sample. However, when chiral sphere is placed on or very near the axis of cavity, we find $\Delta f_{021} > 0$ (e.g., $\xi_c = 3 \times 10^{-3}\Omega^{-1}$). It is clear that $|\Delta f_{mnl}|$ is also dependent on the chiral admittance ξ_c.

Fig. 3 illustrates $\frac{\Delta f_{021}}{f_{021}}$ as a function of ρ_0/R_2 for the chiral sphere of "large size".

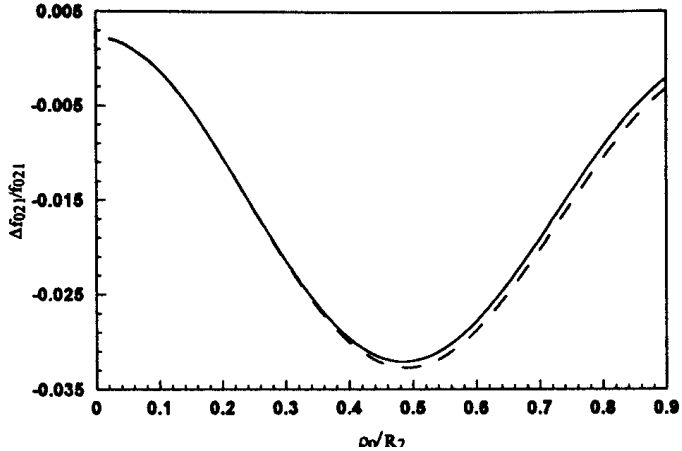

Figure 3. As in Fig. 2, except that $R_1/R_2 = 0.2$, $\xi_c = 3 \times 10_{-3}\Omega_{-1}$ (one-order: ——; three-order: – – –).

It is observed that, for chiral sample of "large size", the calculated result from (26) is exact as that from two- or three-order modified formulas (27)–(29) only when the sample is placed not far from the axis of cavity. But, when $\rho_0 \to 0, |\Delta f_{021}|$ becomes very small, this is disadvantageous for measuring the constitutive parameters of chiral samples. The best place for chiral sample of "large size" is the point on which the resonant frequency shift reaches the maximum value.

Furthermore, Figs. 4 and 5 depict $\frac{\Delta f_{mnl}}{f_{mnl}}$ versus ρ_0/R_2 for some different TE and TM $_{mnl}$ modes, respectively.

In Figs. 4 and 5, R_1/R_2 is chosen to be 0.1 and all computed data are obtained from (29) by taking account of higher-order resonant frequency shifts. It is shown that the resonant frequency shifts for TE $_{mnl}$ and TM $_{mnl}$ modes are always $\Delta f_{mnl} < 0$ for the given constitutive parameters. Especially, for TE $_{111}$, TE $_{121}$ and TM $_{010}$,TM $_{112}$ modes the magnitudes of $|\Delta f_{mnl}|$ are the largest when $\rho_0 = 0$

Fig. 6 shows $\frac{\Delta f_{mnl}}{f_{mnl}}$ versus z_0/H for TM $_{010}$ and TM $_{012}$ corresponding different chiral admittances.

In Fig. 6, the resonant frequency shift Δf_{010} keeps constant with z_0/H changing. Such feature has no relation to chiral admittance only because of $l = 0$, and this phenomenon is similar to non-chiral

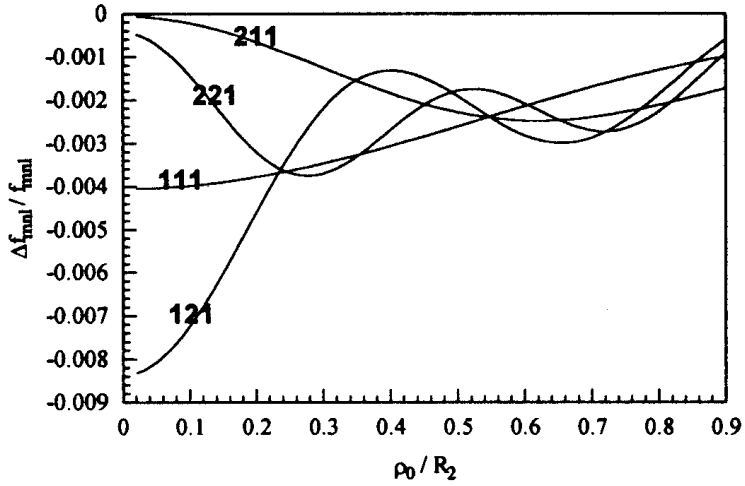

Figure 4 $\frac{\Delta f_{mnl}}{f_{mnl}}$ versus ρ_0/R_2 for TE $_{mnl}$ mode in a perfectly conducting cylindrical cavity with a chiral sphere: $R_1/R_2 = 0.1$, $R_2/H_2 = 1.0$, $z_0/H = 0.6$, $\varepsilon = 3.5\varepsilon_0$, $\mu = 1.2\mu_0$, $\xi_c = 3 \times 10^{-3}\Omega^{-1}$.

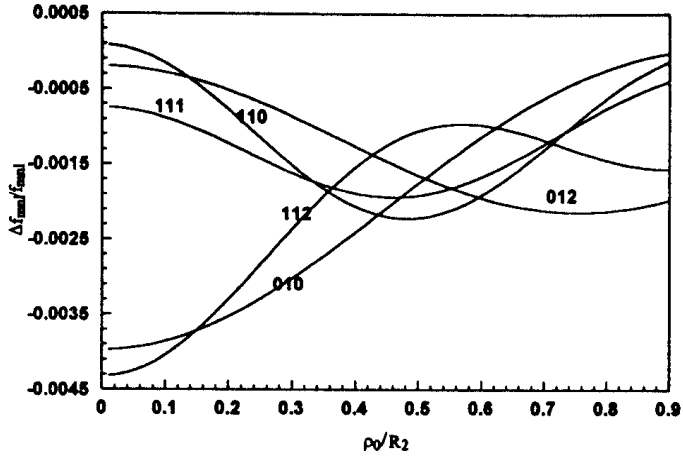

Figure 5. $\frac{\Delta f_{mnl}}{f_{mnl}}$ versus ρ_0/R_2 for TE $_{mnl}$ mode in a perfectly conducting cylindrical cavity with a chiral sphere: $R_1/R_2 = 0.1$, $R_2/H_2 = 1.0$, $z_0/H = 0.2$, $\varepsilon = 3.5\varepsilon_0$, $\mu = 1.2\mu_0$, $\xi_c = 3 \times 10^{-3}\Omega^{-1}$.

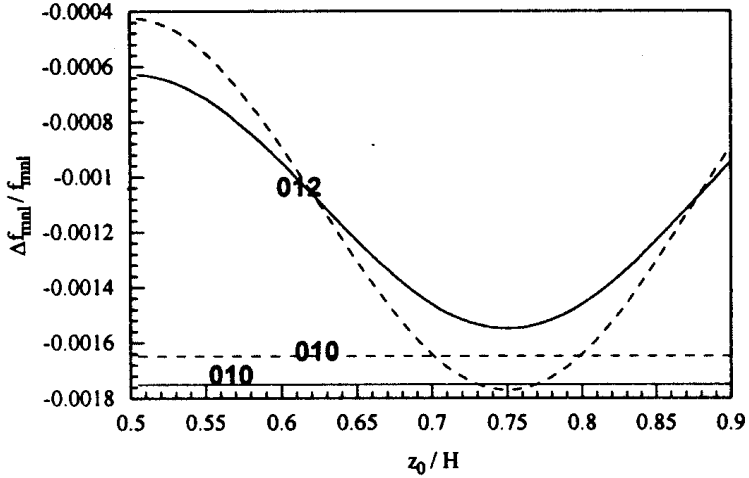

Figure 6. $\frac{\Delta f_{mnl}}{f_{mnl}}$ versus z_0/H in a perfectly conducting cylindrical cavity with a chiral sphere: $R_1/R_2 = 0.1$, $R_2/H_2 = 1.0$, $\rho_2/R_2 = 0.5$, $\varepsilon = 3.5\varepsilon_0$, $\mu = 1.2\mu_0$, $\xi_c = 0$ (——); $10^{-3}\Omega^{-1}$ (– – –); $3 \times 10^{-3}\Omega^{-1}$ (- - - -).

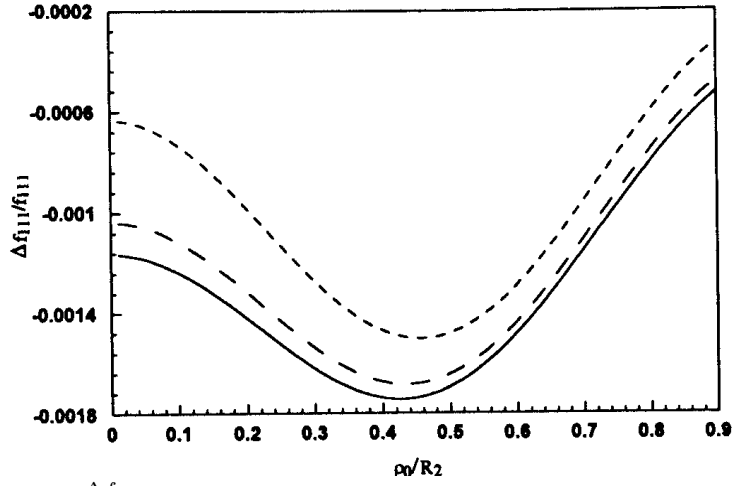

Figure 7. $\frac{\Delta f_{111}}{f_{111}}$ versus ρ_0/R_2 for TM_{011} in a perfectly conducting cylindrical cavity with a (non)reciprocal chiral sphere: $R_1/R_2 = 0.1\, R_2/H_2 = 1.0, z_0/H = 0.2, \varepsilon = 3.5\varepsilon_0, \mu = 1.2\mu_0, \chi = 0, \kappa = 0.5\sqrt{\mu_0\varepsilon_0}$ (——); $\chi = \kappa = 0.5\sqrt{\mu_0\varepsilon_0}$ (– – –); $\chi = 2\kappa = \sqrt{\mu_0\varepsilon_0}$ (- - - -).

case [23]. As ξ_c increases continuously, Δf_{010} tends towards positive shift. For TM_{012} mode, the oscillation is enhanced greatly with ξ_c increasing.

Finally, Fig. 7 depicts the combined effect of nonreciprocity and chirality parameters on the resonant frequency shift of TM_{011} mode in a cylindrical cavity.

It is shown that the magnitude of relative resonant frequency shift decreases with the increasing of χ or κ and tends to positive shift.

Correspondingly, similar phenomena can be observed for the influences of chirality on the resonant frequency shift of different modes in a spherical cavity.

6. CONCLUSIONS

We have investigated the resonant features of a perfectly conducting cylindrical and spherical cavities with a biisotropic (non)reciprocal chiral sphere by means of boundary-value technique, and not only the first-order but also the second- and third- order perturbational contributions are considered. It is believed that the formulas presented above have certain advantages since both "small" and "large" size are applicable, so it can be directly used for characterizing the constitutive parameter of chiral samples. On the other hand, the study above can be easily extended to the case of small biisotropic (non)reciprocal chiral sample of other shapes following the similar procedure developed above, and are also useful in developing cavity technique for measuring of the constitutive characteristics of bianisotropic materials.

ACKNOWLEDGMENT

The author (W. Y. Yin) appreciates the Alexander von Humboldt Research Foundation of Germany greatly for sponsorship of this research and Prof. Ingo Wolff's valuable suggestions.

APPENDIX 1

In (7), (8), (40), and (41),

$$
\begin{aligned}
A_{\mu-m,v} &= \frac{1}{2}(-1)^{\mu-m} J_{\mu-m}(k_{mn}\rho_0) e^{-i(\mu-m)\varphi_0} \frac{2v+1}{v(v+1)} \frac{(v-\mu)!}{(v+\mu)!} i^{v-\mu} \\
&\quad \cdot k_{mnl}(e^{ik_{zl}z_0} + (-1)^{v+\mu} e^{-ik_{zl}z_0}) \sin\alpha \frac{dP_v^\mu(\cos\alpha)}{d\alpha} \\
B_{\mu-m,v} &= \frac{1}{2}(-1)^{\mu-m} J_{\mu-m}(k_{mn}\rho_0) e^{-i(\mu-m)\varphi_0} \frac{2v+1}{v(v+1)} \frac{(v-\mu)!}{(v+\mu)!} i^{v-\mu} \\
&\quad \cdot k_{mnl}(e^{ik_{zl}z_0} - (-1)^{v+\mu} e^{-ik_{zl}z_0})(m+n) P_v^\mu(\cos\alpha) \\
A'_{\mu-m,v} &= \frac{i}{2}(-1)^{\mu-m} J_{\mu-m}(k'_{mn}\rho_0) e^{-i(\mu-m)\varphi_0} \frac{2v+1}{v(v+1)} \frac{(v-\mu)!}{(v+\mu)!} i^{v-\mu} \\
&\quad \cdot k'_{mnl}(e^{ik'_{zl}z_0} - (-1)^{v+\mu} e^{-ik'_{zl}z_0}) \sin\alpha \frac{dP_v^\mu(\cos\alpha)}{d\alpha} \\
B'_{\mu-m,v} &= \frac{i}{2}(-1)^{\mu-m} J_{\mu-m}(k'_{mn}\rho_0) e^{-i(\mu-m)\varphi_0} \frac{2v+1}{v(v+1)} \frac{(v-\mu)!}{(v+\mu)!} i^{v-\mu} \\
&\quad \cdot k'_{mnl}(e^{ik'_{zl}z_0} + (-1)^{v+\mu} e^{-ik'_{zl}z_0})(m+n) P_v^\mu(\cos\alpha)
\end{aligned}
\tag{A1}
$$

APPENDIX 2

In (16) and (17),

$$
\begin{aligned}
D_{1n'} &= [(1+\eta)(\eta j j_- \partial j_+ \partial h + j_+ h \partial j \partial j_- - j_+ j_- \partial j \partial h) \\
&\quad +(1-\eta)(-\eta j j_+ \partial j_- \partial h + j_- h \partial j \partial j_+ + j_+ j_- \partial j \partial h) \\
&\quad -2\eta j h \partial j_+ \partial j_-]/\Delta \\
D_{2n'} &= [(1+\eta)(\eta j_+ h \partial j \partial j_- - j h \partial j_+ \partial j_- + j j_- \partial j_+ \partial h) \\
&\quad +(1-\eta)(-\eta j_- h \partial j \partial j_+ + j h \partial j_+ \partial j_- + j j_+ \partial j_- \partial h) \\
&\quad -2\eta \partial j \partial h j_+ j_-]/\Delta \\
D_{3n'} &= [(1+\eta)(\eta j j_+ \partial j_- \partial h + j_- h \partial j \partial j_+ \\
&\quad +(1-\eta)(j_+ h \partial j \partial j_- - \eta j j_- \partial j_+ \partial h) \\
&\quad -2\eta(\partial j \partial h j_+ j_- + j h \partial j_+ \partial j_-)]/\Delta
\end{aligned}
$$

$$
\begin{aligned}
D_{4n'} &= [(1+\eta)(-\eta j_- h\partial j_+ \partial j - j j_+ \partial j_- \partial h) \\
&\quad + (1-\eta)(\eta j_+ h \partial j \partial j_- - j j_- \partial j_+ \partial h) \\
&\quad + 2\eta(\partial j \partial h j_+ j_- + j h \partial j_+ \partial j_-)]/\Delta \\
\Delta &= 2[2\eta(j_+ j_- \partial h^2 + \partial j_+ \partial j_- h^2) - \eta^2 h \partial h (j_+ \partial j_- + j_- \partial j_+)]
\end{aligned}
\tag{A2}
$$

where the subscript n' of spherical Bessel and Hankel functions and their derivatives is omitted. When $x = k_{mn}R_1 (x_\pm = k_{mnl\pm}R_1) < 1$ we have

$$
\begin{aligned}
& j \approx \frac{x^{n'}}{1\cdot 3\cdot 5\cdots(2n'+1)},\ j_\pm \approx \frac{x_\pm^{n'}}{1\cdot 3\cdot 5\cdots(2n'+1)} \\
& \partial j \approx \frac{x^{n'-1}(n'+1)}{1\cdot 3\cdot 5\cdots(2n'+1)},\ \partial j_\pm \approx \frac{x_\pm^{n'-1}(n'+1)}{1\cdot 3\cdot 5\cdots(2n'+1)} \\
& h \approx -i\frac{1\cdot 3\cdot 5\cdots(2n'-1)}{x^{n'+1}}, \quad h_\pm \approx -i\frac{1\cdot 3\cdot 5\cdots(2n'-1)}{x_\pm^{n'+1}} \\
& \partial h \approx i\frac{1\cdot 3\cdot 5\cdots(2n'-1)n'}{x^{n'+2}}, \quad \partial h_\pm \approx i\frac{1\cdot 3\cdot 5\cdots(2n'-1)n'}{x_\pm^{n'+2}} \\
& \text{and} \qquad h\partial j - j\partial h = -\frac{i}{x^2}
\end{aligned}
\tag{A3}
$$

APPENDIX 3

$$\begin{aligned}
\iint \vec{B}_{-2,2} \cdot \vec{B}^*_{-2,2} d\Omega &= \iint \vec{C}_{-2,2} \cdot \vec{C}^*_{-2,2} d\Omega = \frac{\pi}{30}, \\
\iint \vec{B}_{-1,2} \cdot \vec{B}^*_{-1,2} d\Omega &= \iint \vec{C}_{-1,2} \cdot \vec{C}^*_{-1,2} d\Omega = \frac{2\pi}{15}, \\
\iint \vec{B}_{0,2} \cdot \vec{B}^*_{0,2} d\Omega &= \iint \vec{C}_{0,2} \cdot \vec{C}^*_{0,2} d\Omega = \frac{4\pi}{5}, \\
\iint \vec{B}_{1,2} \cdot \vec{B}^*_{1,2} d\Omega &= \iint \vec{C}_{1,2} \cdot \vec{C}^*_{1,2} d\Omega = \frac{24\pi}{5}, \\
\iint \vec{B}_{2,2} \cdot \vec{B}^*_{2,2} d\Omega &= \iint \vec{C}_{2,2} \cdot \vec{C}^*_{2,2} d\Omega = \frac{96\pi}{5}, \\
\iint \vec{B}_{-3,3} \cdot \vec{B}^*_{-3,3} d\Omega &= \iint \vec{C}_{-3,3} \cdot \vec{C}^*_{-3,3} d\Omega = \frac{\pi}{1260}, \\
\iint \vec{B}_{-2,3} \cdot \vec{B}^*_{-2,3} d\Omega &= \iint \vec{C}_{-2,3} \cdot \vec{C}^*_{-2,3} d\Omega = \frac{\pi}{210}, \\
\iint \vec{B}_{-1,3} \cdot \vec{B}^*_{-1,3} d\Omega &= \iint \vec{C}_{-1,3} \cdot \vec{C}^*_{-1,3} d\Omega = \frac{\pi}{21}, \\
\iint \vec{B}_{0,3} \cdot \vec{B}^*_{0,3} d\Omega &= \iint \vec{C}_{0,3} \cdot \vec{C}^*_{0,3} d\Omega = \frac{4\pi}{7}, \\
\iint \vec{B}_{1,3} \cdot \vec{B}^*_{1,3} d\Omega &= \iint \vec{C}_{1,3} \cdot \vec{C}^*_{1,3} d\Omega = \frac{48\pi}{7}, \\
\iint \vec{B}_{2,3} \cdot \vec{B}^*_{2,3} d\Omega &= \iint \vec{C}_{2,3} \cdot \vec{C}^*_{2,3} d\Omega = \frac{480\pi}{7}, \\
\iint \vec{B}_{3.3} \cdot \vec{B}^*_{3,3} d\Omega &= \iint \vec{C}_{3,3} \cdot \vec{C}^*_{3,3} d\Omega = \frac{2880\pi}{7},
\end{aligned} \tag{A4}$$

REFERENCES

1. Cory, H., "Chiral devices–an overview of canonical problems," *J. Electromagn. Waves and Appl.*, Vol. 9, No. 5/6, 805–829, 1995.
2. Mahmoud, S. F., "Characteristics of a chiral-coated slotted cylindrical antenna," *IEEE Trans. Antennas and Propagat.*, Vol. 44, No. 7, 814–821, 1996.
3. Qiu , R. C., and I.-T. Lu,"Guided waves in chiral optical fibers," *J. Opt. Soc. Am. A.*, Vol. 11, No. 12, 3212–3219, 1994.

4. Saadoun, M. M. I., and N. Engheta, "Theoretical study of variation of propagation constant in a cylindrical waveguide due to chirality: chiro-phase shifting," *IEEE Trans. Microwave Theory and Tech.*, Vol. 42, No. 9, 1690–1694, 1994.
5. Luebbers, R., H. S. Langdon, F. Hunsberger, C. F. Bohren, and S. Yoshikawa, "Calculation and measurement of the effective chirality parameter of a composite chiral material over a wide frequency band," *IEEE Trans. Antennas and Propagat.*, Vol. 43,No. 2, 123–129, 1995.
6. Whites, K. W., "Full-wave computation of constitutive parameters for lossless composite chiral materials," *IEEE Trans. Antennas and Propagat.*, Vol. 43, No. 4, 376–384, 1995.
7. Bahr, A. J., and K. R. Clausing, "An approximate model for artificial chiral material," *IEEE Trans. Antennas and Propagat.*, Vol. 42, No. 12, 1592–1596, 1994.
8. Oberschmidt, G., and A. F. Jacob, "Averaging rules for the scattering by randomly oriented chiral particles," *IEEE Trans. Microwave Theory and Tech.*, Vol. 44, No. 3, 476–478,1996.
9. Tretyakov, S. A., F. Mariotte, C. R. Simovski, T. G. Kharina, and J. P. Heliot, "Analytical antenna model for chiral scatterers:comparision with numerical and experimental data," *IEEE Trans. Antennas and Propagat.*, Vol. 44, No. 7, 1006–1014, 1996.
10. Lakhtakia, A., V. K. Varadan, and V. V. Varadan, "Dilute random distribution of small chiral spheres," *Appl. Opt.*, Vol. 29, No. 25, 3627–3632, 1990.
11. Sihvola, A. H., "Bi-isotropic mixtures," *IEEE Trans. Antennas and Propagat.*, Vol. 40, No. 2, 188–197, 1992.
12. Zhuck, N. P., and A. S. Omer, "Calculation of the effective constitutive parameters of a disorded bi-isotropic medium using renormalization method," *IEEE Trans. Antennas and Propagat.*, Vol. 44, No. 8, 1142–1149, 1996.
13. Hollinger, R. D., V. V. Varadan, and V. K. Varadan,"Eigenmodes in a circular waveguide containing an isotropic chiral material," *Radio Science*, Vol. 26, No. 5, 1335–1344, 1991.
14. Varadan, V. V., R. Rao, and V. K. Varadan, "Measurement of the electromagnetic properties of chiral composite materials in the 8-40 GHz range," *Radio Science*, Vol. 29, No. 1, 9–22, 1994.
15. Guerin, F., V. K. Varadan, and V. V. Varadan, M. Labeyrie, and P. Y. Cuillon, "Some experimental results on the dispersive behaviour of chiral composites," *J. Phys. D: Appl. Phys.*, Vol. 28, 194–201, 1995.

16. Theron, J. P., and J. H. Cloete, "The electric quadrupole contribution to the circular birefringence of nonmagnetic anisotropic chiral media:circular waveguide experiment," *IEEE Trans. Microwave Theory and Tech.*, Vol. 44, No. 8, l451–1459, 1996.
17. Mariotte, F., and N. Engheta, "Reflection from a lossy chiral slab (with and without metallic backing)in a parallel plate waveguide, "*Radio Science*, Vol. 30, No. 4, 827–834, 1995.
18. Tretyakov, S. A., and D. Y. Haliullin, "Free-space technique for biisotropic media parameter measurement," *Micro. Opt. Tech. Lett.*, Vol. 6, No. 8, 512–515, 1993.
19. Lakhtakia, A., "Perturbation of a resonant cavity by a small bianisotropic sphere," *Int. J. Infrared and Millimeter Waves,* Vol. 12, No. 2, 109–114,1991.
20. Tretyakov, S. A., and A. J. Viitanen, "Perturbation theory for a cavity resonator with a biisotropic sample:applications to measurement technique," *Micro. Opt. Tech. Lett.*, Vol. 5, No. 2, 174–177, 1992.
21. Viitanen, A. J., and I. V. Lindell, "Perturbation theory for a corrugated waveguide with a bi-isotropic rod," *Micro. Opt. Tech. Lett.*, Vol. 5, No. 4, 729–732, 1992.
22. Tretyakov, S. A., and A. J. Viitanen, "Waveguide and resonator perturbation technique measuring chiralty and nonreciprocity parameters biisotropic materials," *IEEE Trans. Microwave Theory and Tech.*, Vol. 43, No. 1, 222–225, 1995.
23. Roumeliotis, J. A., "Resonant frequencies in an electromagnetic cylindrical cavity with an internal off-axis small sphere," *J. Electromagn. Waves and Appl.*, Vol. 6, No. 11, 1581–1600, 1992.
24. Roumeliotis, J. A., J. D. Kanellopoulos, and J. G. Fikioris, "Resonant frequencies in an electromagnetic spherical cavity with an eccentric inner electrically small sphere," *Electromagnetics*, Vol. 12, No. 2, 155–170, 1992.
25. Roumeliotis, J. A., and G. Kokkorakis, "Resonant frequencies in an electromagnetic cylindrical/spherical cavity with an internal off-axis small dielectric sphere," *Electromagnetics*, Vol. 14, 195–215, 1994.
26. Rao, T. C. K., "Resonant frequency and Q-factor of a cylindrical cavity containing an chiral medium,"*Int. J. Electronics,* Vol. 73, No. 1, 183–191, 1992.
27. Xu, Y., and R. Bosisio, "Calculation of dielectric resonators with complicated constitutive parameters," *IEE Proc. Microw. Antennas Propagat.*, Vol. 142, No. 6, 477–480, 1995.

28. Lakhtakia, A., V. V. Varadan, and V. K. Varadan, "Eigenmodes of a chiral sphere with a perfectly conducting coating," *J. Phys. D: Appl. Phys.*, Vol. 22, 828–825, 1989.
29. Engheta, E., and M. W. Kowarz, "Antenna radiation in the presence of a chiral sphere,"*Appl. Phys.*, Vol. 67, No. 2, 639–646, 1990.
30. Yin,W. Y., W. Wang, and P. Li, "Dyadic Green's function in arbitrary spherical chiral media and its applications;" *J. Electromagn. Waves and Appl.,* Vol. 9, No. 1/2, 157–173, 1995.
31. Fuller, K. A., "Scattering and absorption cross section of compounded spheres. I. Theory for external aggregation," *J. Opt. Soc. Am. A.*, Vol. 11, No. 12, 3251–3260, 1994.
32. Monzon, J. C., "Radiation and scattering in homogeneous general biisotropic regions," *IEEE Trans. Antennas and Propagat.*, Vol. 36, No. 2, 481–485, 1990.
33. Lindell, I. V., and A. J. Viitanen, "Duality transformations for general biisotropic (non-reciprocal chiral) media," *IEEE Trans. Antennas and Propagat.*, Vol. 40, No. 1, 91–95, 1992.
34. Lindell,I. V., A. H. Sihvola, S. A. Tretyakov, and A. J. Viitanen, *Electromagnetic Waves in Chiral and Bi-isotropic Media*, Artech House, Boston, 1994.
36. Sihvola, A. H., "Bi-isotropic constitutive relations," *IEEE Trans. Antennas and Propagat.*, Vol. 40, No. 2, 188–197, 1992.
37. Lindell, I. V., P. K. Koivisto, S. A. Tretyakov, and M. I. Oksanen, "Waveguide filled with general biisotropic media," *Radio Science,* Vol. 28, No. 5, 675–686, 1993.
38. Yin, W. Y., W. B. Wang, and P. Li, "The theory of dyadic Green's function and the radiation characteristics of sources in multilayered biisotropic media," *Progress in Electromagnetics Research*, PIER9, 117–135, 1994.